



# Effects of non-reflection events and stationary sources locations on virtual seismic reflection images

Ki Young Kim<sup>1</sup>\*, Youngseok Song<sup>2</sup>) and Joongmoo Byun<sup>2</sup>)

(1) Kangwon National University, Geophysics, Chunchon, Korea, Republic Of(South) \*kykim@kangwon.ac.kr,  
(2) Hanyang university, Earth Resources and Environmental Engineering, Seoul, Korea, Republic Of (South)



## 1. Abstract

To notice key obstacles and suggest effective processing methods for virtual reflection images, numerical modeling was performed by the 2-D finite difference method with time and space intervals of 0.2 ms and 1.25 m, respectively. Vertical sources of the Ricker wavelet with a main frequency of 20 Hz were assumed to be detonated independently at five buried locations with intervals of 500 m. Vertical components of the particle velocity were computed at 99 receivers at 10 m depth with intervals of 20 m. Synthetic data show that maximum amplitudes of reflection signals are less than 2 % of those of direct Rayleigh waves on an average. This indicates that the non-reflection events should be attenuated as much as possible before correlating traces to compute virtual seismic data. For attenuating both direct and diffracted Rayleigh waves in the synthetic data, a median filter with a time window of a 0.1 s length was effective. Because stationary-phase source locations for virtual reflections concentrate near receiver locations, only common midpoint gathers close to the sources should be used for good virtual stack images.

## 2. Seismic interferometry

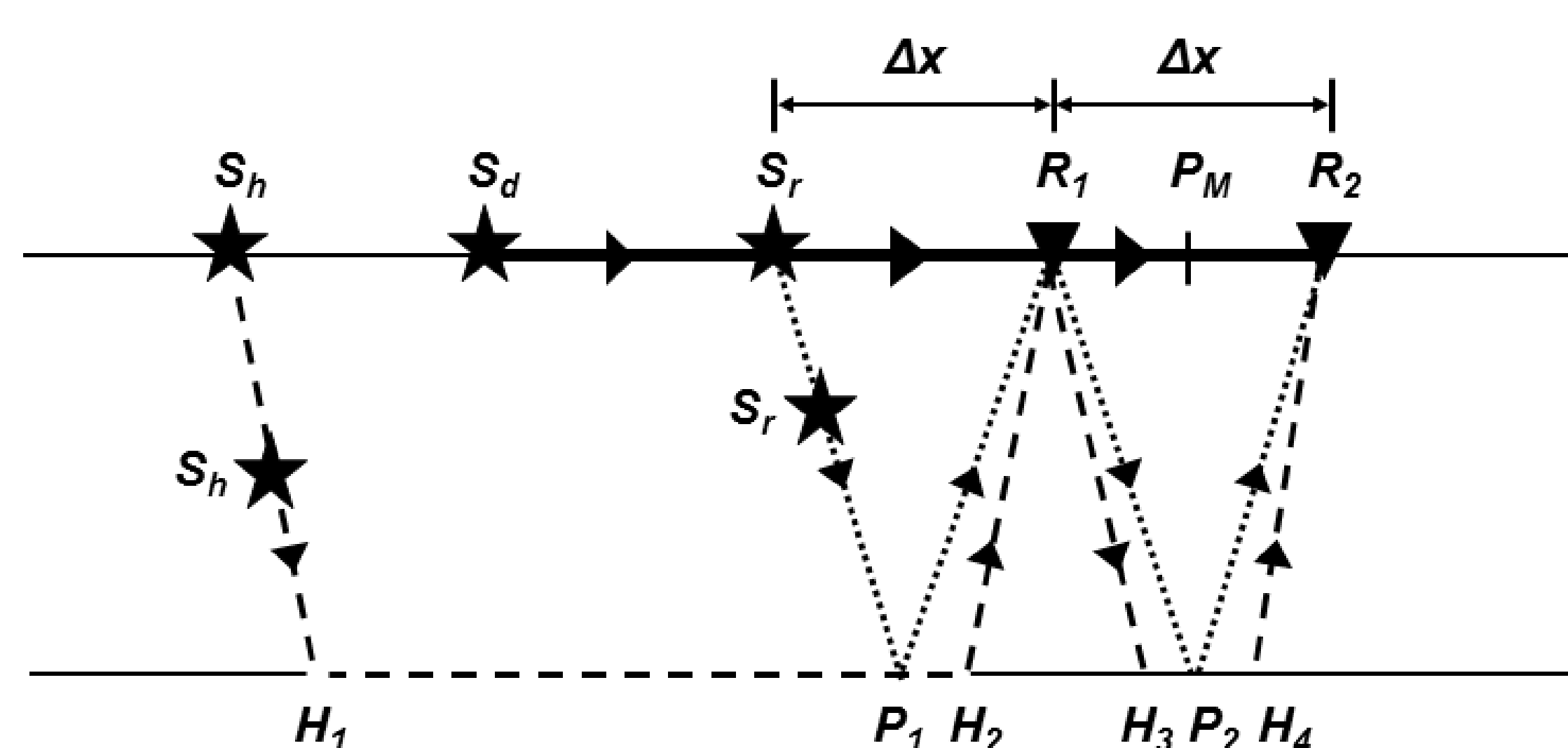


Figure 1. Schematic diagram of raypaths for direct (thick solid), critical refraction (dashed), and reflection (dotted) interferometry with two receivers,  $R_1$  and  $R_2$  (triangles), in a homogeneous two-layer layer model. Stationary source locations (stars) can be in any position along the profile away from the two receivers for the direct waves ( $S_d$ ), farther than the critical distance from the nearer receiver for the critically refracted waves ( $S_h$ ), and only at the distance equal to the separation of paired receivers ( $\Delta x$ ) from the nearer receiver ( $S_r$ ) and its multiples for reflected waves. Buried stationary source locations ( $S_h$  and  $S_r$ ) and midpoint ( $P_M$ ) are also indicated (modified from Song et al, 2018).

$$G(X_{R_2}, X_{R_1}, t) * A_S(t) = w(X_{R_2}, X_S, t) \otimes w(X_{R_1}, X_S, t)$$

For the case of a seismic direct wave proceeding from the source,  $S_d$ , through one receiver,  $R_1$ , and traveling on to a second receiver,  $R_2$ , along the surface (Fig. 1), cross-correlation of the observed signals at the positions of  $X_{R_2}$  and  $X_{R_1}$  produces a one-dimensional Green's function when the virtual source and receiver are located at  $X_{R_1}$  and  $X_{R_2}$ , respectively.  $\Phi_S(t)$  is the autocorrelation function of a source wavelet and  $u(t)$  is the convolution of the Green's function and the source wavelet.

## 3. Synthetic Model and Shot Gathers

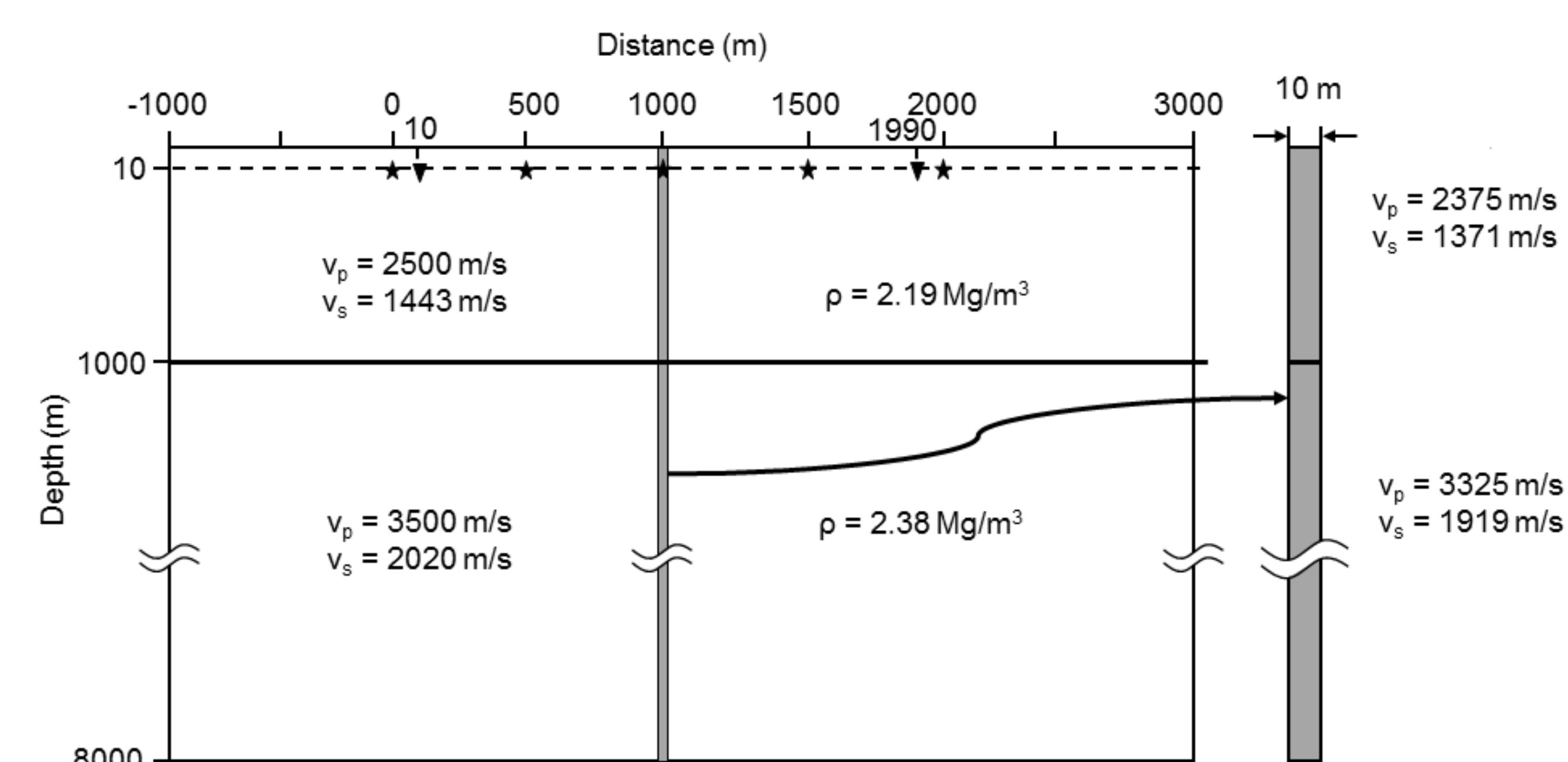


Figure 2. Synthetic model used for this seismic reflection interferometry (SRI) study. Seismic energy independently generated at five sources (stars) at 10 m depth was assumed to be recorded at 99 active receivers (triangles) buried at the same depth as the sources. The 10-m thick vertical boundary (gray) in the middle of the profile is horizontally exaggerated and illustrated at the right of the model.

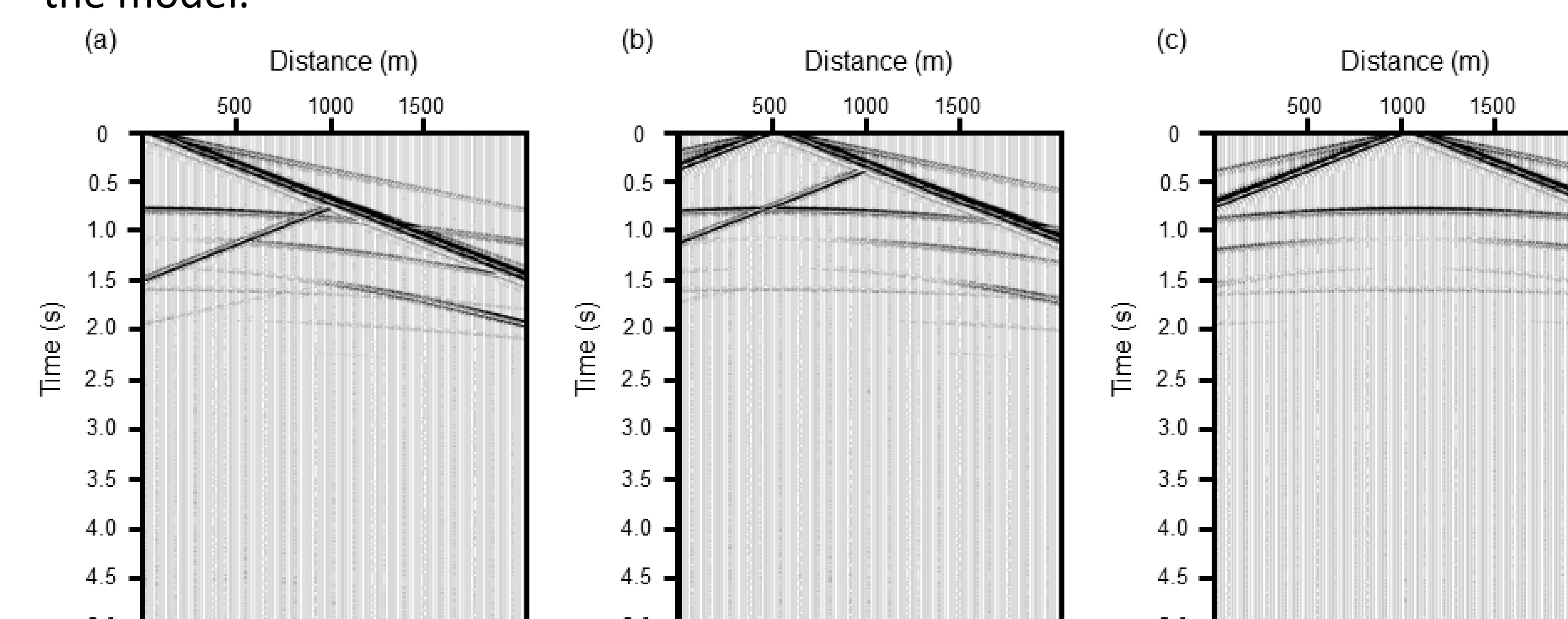


Figure 3. Synthetic source gathers (SSGs) at (a) 0, (b) 500, and (c) 1000 m from the origin. By symmetry, SSGs at 1500 and 2000m are simply mirror images of SSGs at 500 and 0 m, respectively.

## 4. Data Processing

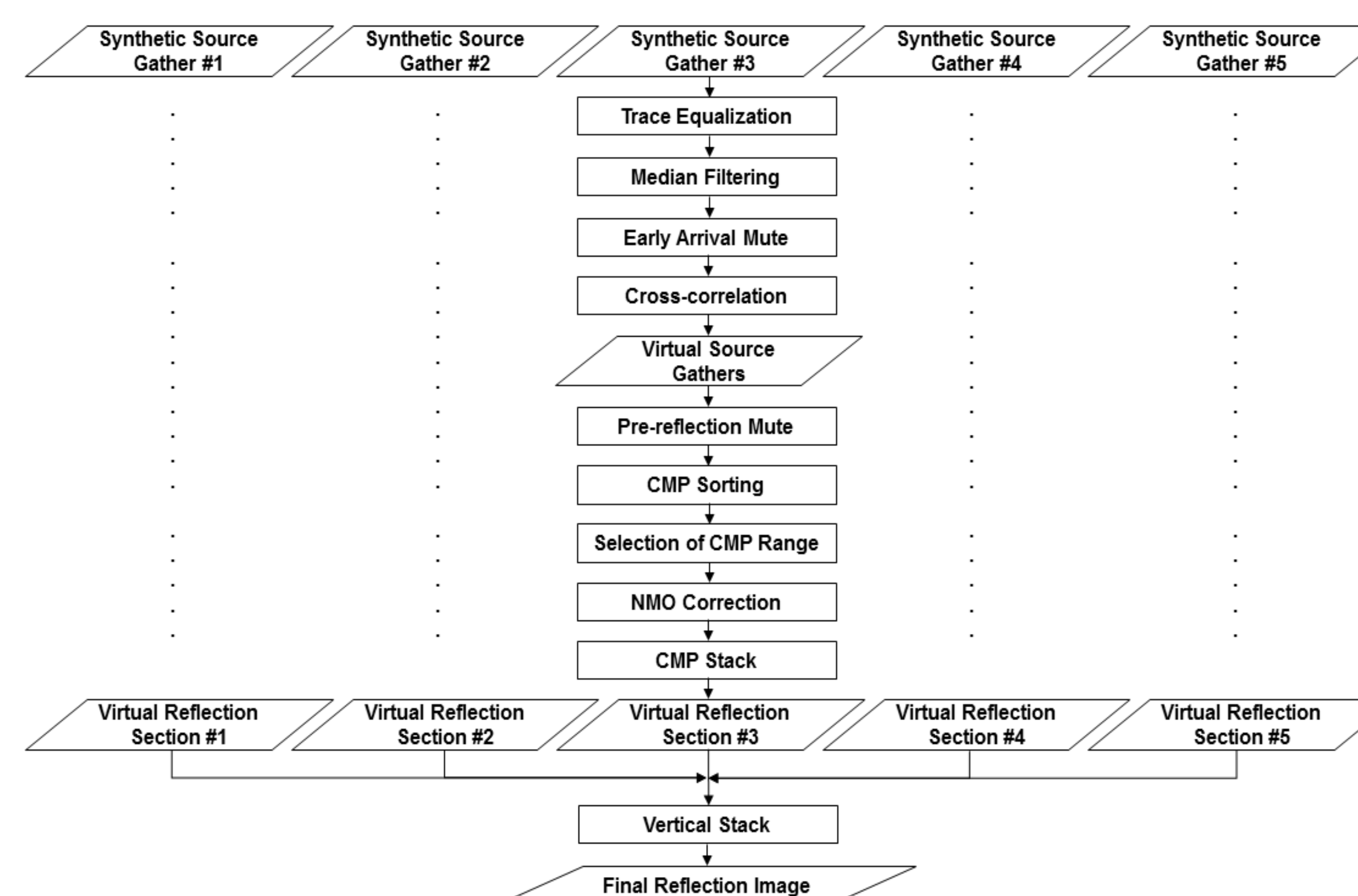


Figure 4. Processing flow for the SRI image.

## 5. SSGs and VSGs

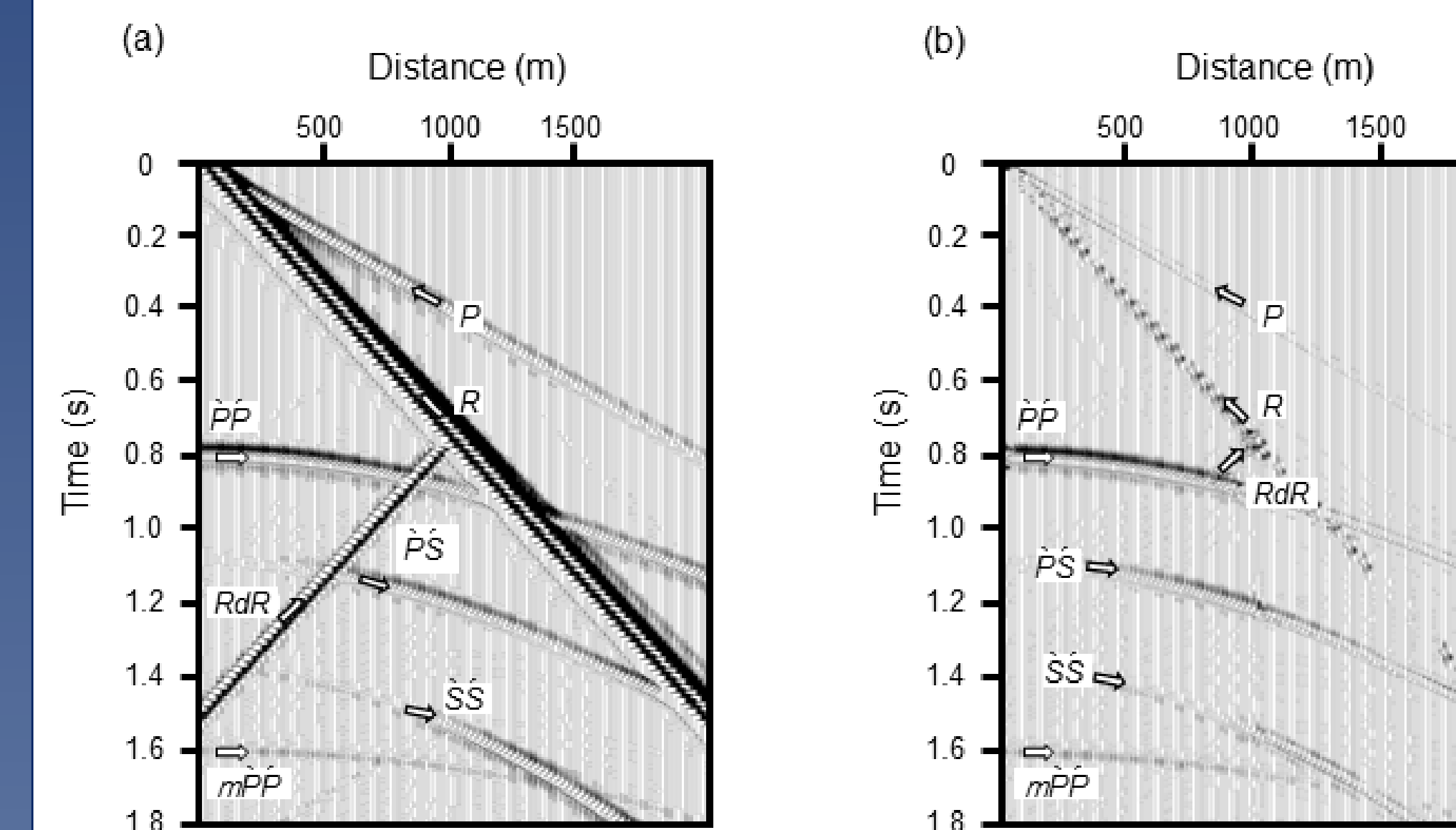


Figure 5. Synthetic source gathers (SSGs) (a) before and (b) after applying the median filter. Strong linear events comprise both direct P (P) and R (R) waves, and diffracted R (RdR) waves with a negative slope. Reflections of P (P'), converted (P'S'), and S (S') waves are hyperbolic. After applying the median filter (b), however, both direct and diffracted R waves were greatly attenuated.

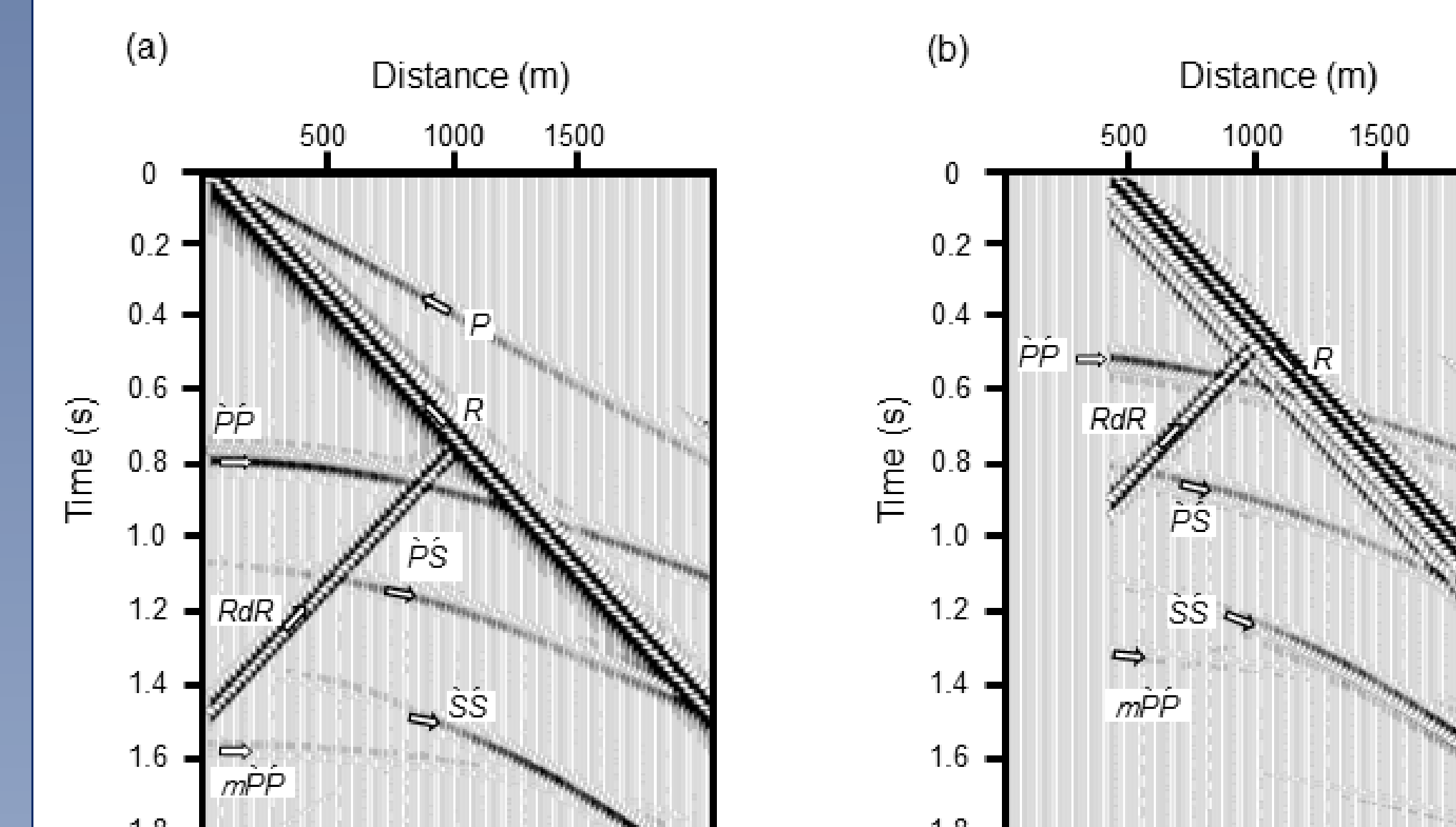


Figure 6. Virtual source gathers without the preprocess for attenuating non-reflection events at (a) the nearest active receiver location and (b) a distance of 410 m from the origin. The near-offset traces (at distances less than 30 m) in (b) are null since the farther receivers of receiver pairs can not serve as virtual sources..

## 6. Conclusions

- In this SI model, the amplitude of Rayleigh waves (R and RdR) is 60 times stronger on average than the amplitude of the reflected waves, and that the relative amplitude of the P'P' and mP'P' phase used to obtain the virtual reflected wave signals is very weak at 1.3% and 0.2%, respectively. This is the main reasons why the virtual reflected imaging method has not widely applied in practice. Therefore, attenuation of R and RdR phases prior to the cross-correlation process is essential for SRI images of high S/N ratios.
- The optimum range of CMP to be horizontally stacked should be determined based on two criteria; one is the proximity of virtual CMP locations from the source for large reflectivities, and the other is wider range to increase CMP folds.

## 7. Acknowledgement

This work was supported by the Human resources Development program (No. 20164010201120) of the Korea Institute of Energy Technology Evaluation and Planning (KETEP) grant funded by the Korea Ministry of Trade, Industry and Energy. One of the author, Youngseok Song, was supported by NRF (National Research Foundation of Korea) grant funded by the Korea government (NRF-2017H1A2A1044244-Global Ph. D. Fellowship Program)

## 6. Stacked Section

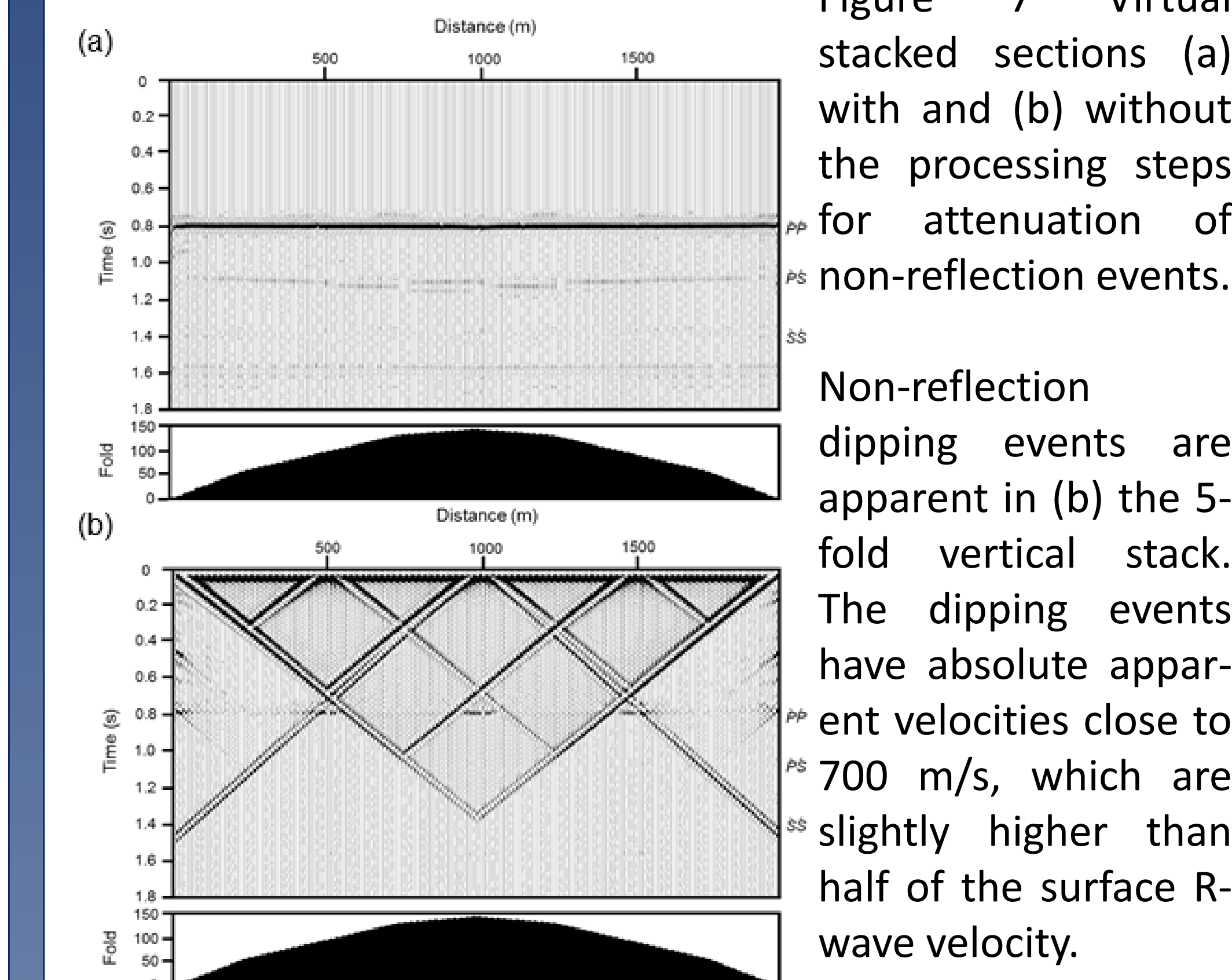


Figure 7. Virtual stacked sections (a) with and (b) without the processing steps for attenuation of non-reflection events.

Non-reflection dipping events are apparent in (b) the 5-fold vertical stack. The dipping events have absolute apparent velocities close to 700 m/s, which are slightly higher than half of the surface R-wave velocity.

## 7. Instantaneous amplitudes

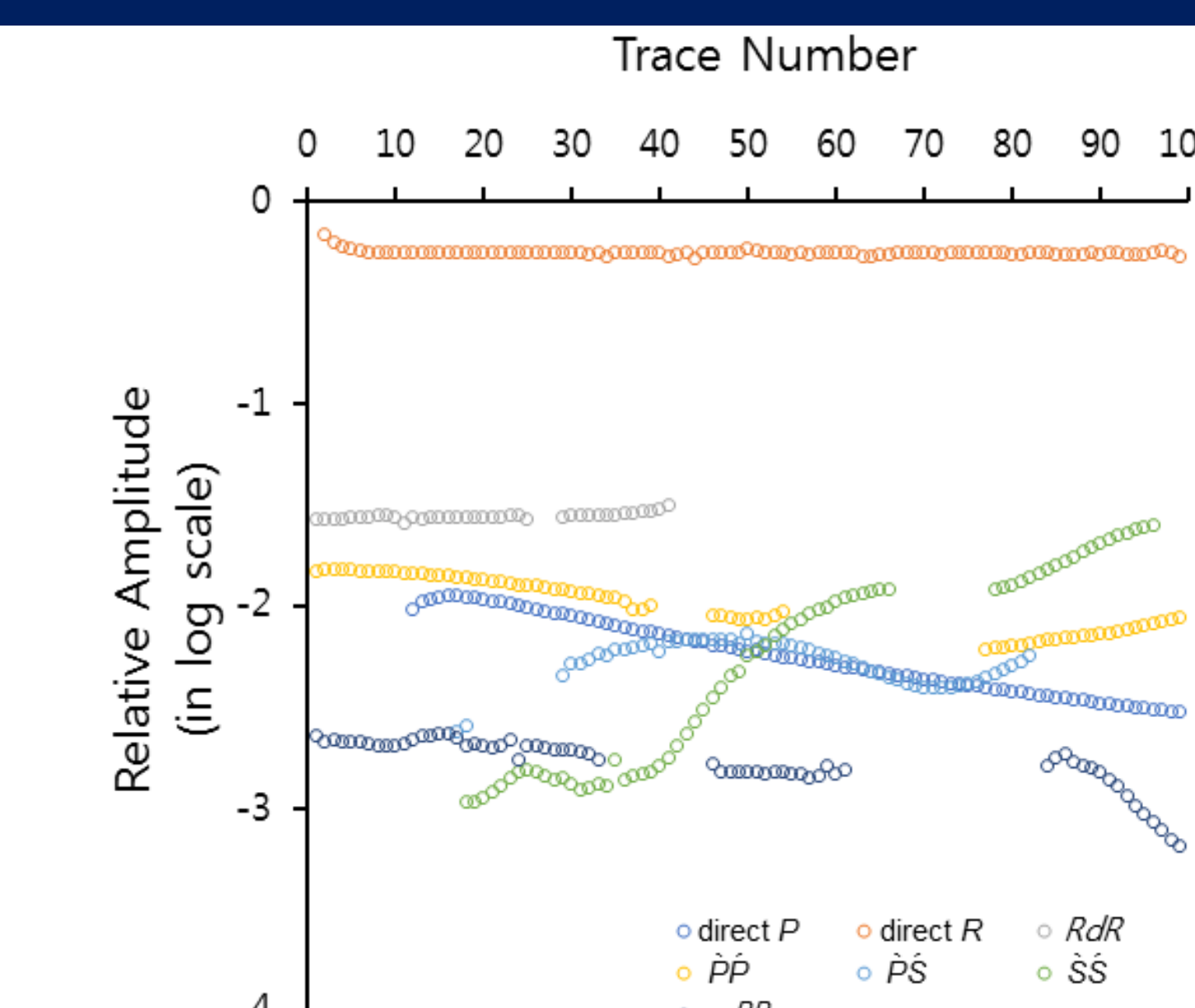


Figure 8. Instantaneous amplitudes of various phases in the synthetic seismic data for the source at the origin. Notice that the vertical axis is in the logarithmic scale. Direct R wave (orange circles) is much stronger than the P'P' reflection (yellow circles) event.